Batteries & Supercaps

Research Article
doi.org/10.1002/batt.202300061

Chemistry Europe
European Chemical Societies Publishing

www.batteries-supercaps.org

VIP *Very Important Paper*

Toward Highly Reliable Potassium-Ion Half and Full Coin Cells

Badre Larhrib[a] and Lénaïc Madec*[a, b]

To develop high energy and high-power potassium-ion batteries (KIBs), performance need to be evaluated in full-cells instead of half-cells based on the highly reactive K metal that leads to misinterpretation of the results. However, assembling KIBs full-cells is not trivial as many parameters are critical to the obtained performance. This work demonstrates approaches to assemble reliable K-ion full-cells using graphite and $KVPO_4F_{0.5}O_{0.5}$ based electrodes. First, the optimal separators choice/number and electrolyte choice/volume are determined in half-cells then the optimal electrolyte volume is determined in full-cells. Importantly, the electrolyte volume should be fixed to about 4 times the porosity volume for both half- and full-cells. Then, using 3-electrodes cells, the optimal negative/positive (N/P) diameter ratio then the optimal N/P capacity ratio are determined to be 1.16 ± 0.2. Finally, these approaches allow assembling KVPFO//graphite coin-cells with an energy density of about 47 $Wh\,kg_{device}^{-1}$ using a high N/P loading ratio of 4/10 (in $mg_{active\text{-}material}\,cm^{-2}$). Overall, this work can be used as a guide to assemble any KIBs full-cell system and thus paves the way to the determine the best negative/positive materials combination in order to develop efficient KIBs.

Introduction

Potassium-ion batteries (KIBs) are emerging as a possible alternative to Li- and Na-ion batteries in the context of renewable energy development requiring large-scale storage systems for which low cost and abundant materials are required. Indeed, potassium has a high abundance (2.1 wt.% of the Earth's crust) while graphite and Al can be used as negative active material and current collector, respectively. Also, high power batteries are expected due to the low desolvation energy of K^+ (~115 kJ/mol vs. ~155 and ~210 kJ/mol for Na and Li) and small solvated radius of K^+ (~3.6 Å vs. ~4.6 and ~4.8 Å for Na^+ and Li^+) in carbonate electrolytes. However, some drawbacks remain: the high atomic mass of K (39.1 g/mol vs. 23 and 6.9 g/mol for Na and Li), the high Shannon's ionic radius of K^+ (1.38 Å vs. 1.02 and 0.76 Å for Na^+ and Li^+) and possible safety issue (i.e., K plating). Thus, high energy and high power KIBs will be obtained only if the benefits exceed these limitations. To address this challenge, KIBs performance needs to be evaluated in full cells. However, as half-cells results are partially driven by the K metal electrode, it is not trivial to assemble KIBs full-cells. In particular, the K plating/stripping has a relatively low coulombic efficiency (<70%) and high polarization (⩾0.1 V even at low rate) in KPF_6 based carbonate electrolytes,[1] which greatly alters the rate performance and capacity retention evaluation.[2,3] Using KFSI instead (in carbonate electrolytes) generally increases the polarization (at least +0.1 V)[3] due to a higher/better passivation of K metal by a more inorganic solid electrolyte interphase (SEI) based on FSI^- degradation products.[4] Note that the full electrolyte degradation pathways at the K metal surface of the commonly used 0.8 M KPF_6 or KFSI EC:DEC was recently studied experimentally[4] with a perfect agreement with recent theoretical calculation.[5,6] As an alternative to carbonate electrolytes, highly concentrated KFSI DME electrolytes should be preferred in half-cells for its K plating/stripping CE >95%[1] with a stable polarization at low/moderate/high rate.[7,8] Also, K metal aging, i.e., K metal passivation and impedance increase over cycling further limit the performance evaluation,[10] while it remains often neglected in the literature. Finally, the electrolyte reactivity at the K surface forms electrolyte degradation products that migrate to the working electrode where they are deposited (electrodes cross-talk or interaction between electrodes) whatever the electrolyte/electrode are,[4,11,12] so that SEI study should be performed in full-cells. Based on these considerations, it is thus of great interest to master the procedure to go from KIBs half-cells to full-cells. Especially, the K metal preparation, electrolyte volume as well as negative/positive diameter and capacity ratios are critical parameters that are still missing in the KIBs literature but need to be evaluated.

To fill this gap, this work aims to assess the impact of electrolyte volume, negative/positive diameter and capacity ratios on the electrochemical performance (CE, polarization, active materials utilization and capacity retention) in order to assemble highly reliable K-ion full-cells. To do so, graphite and $KVPO_4F_{0.5}O_{0.5}$ based electrodes are selected while 2-electrodes half-cells, then 3-electrodes full-cells and finally 2-electrodes full-cells are used to evaluate the impact of these various parameters on the electrochemical performance. Finally, the approaches followed in this work are used to assembled

[a] B. Larhrib, Dr. L. Madec
Universite de Pau et des Pays de l'Adour
E2S UPPA, CNRS, IPREM, Pau (France)
E-mail: lenaic.madec@univ-pau.fr
[b] Dr. L. Madec
Réseau sur le Stockage Electrochimique de l'Energie
CNRS FR3459, Amiens, France

Supporting information for this article is available on the WWW under https://doi.org/10.1002/batt.202300061

Research Article
doi.org/10.1002/batt.202300061
Chemistry Europe
European Chemical Societies Publishing

KVPFO//graphite coin-cells with high negative/positive loading ratio, i.e., with relatively high energy density. Overall, this work can be used as a guide to assemble any KIBs full-cell system.

Experimental Section

Materials and electrodes preparation

K metal electrodes were prepared from K ingot (Alfa Aesar, 99.95%) as followed: using Teflon tweezers, pieces of K metal were placed then spread (using an 8 cm diameter Teflon roller) between 2 latex gloves (as it is very sticky otherwise). Then, 10 mm diameter K metal disks were punched out (on the latex gloves). The K metal disks were then removed from the latex gloves using Teflon tweezers, then placed on a stainless-steel spacer (1 mm thick, 16 mm diameter) and finally scratched with the back of the tweezers.

Graphite electrodes were prepared following a previously optimized electrode formulation:[10] 425 mg of SLP30 (TIMCAL), 25 mg of C65 (MTI), 40 mg of CMC–Na (Sigma-Aldrich, Mw ~250000) and 10 mg of carboxylate SBR (LITEX LB-420, Synthomer) were mixed (85:5:8:2 weight ratio) in 1 mL distilled water using ball milling (PULVERISETTE 7) at 500 rpm for 1 h. Slurry was coated on aluminum foil (15 μm thickness) by doctor blade (125 or 250 μm corresponding to 2 or 4 $mg_{graphite}\,cm^{-2}$). The film was then dried at room temperature for 1 night under air. Then, 11 or 12.7 mm diameter electrodes were cut out, pressed at 2 tons/cm^2 (leading to ~35% electrode porosity) and dried again under vacuum at 80 °C for 12 h.

$KFPO_4F_{0.5}O_{0.5}$ (KVPFO) was synthetized following the procedure reported by Wernert et al.[13] KVPFO electrodes were prepared by mixing 1 g of KVPFO, 0.2 g of C65 (MTI), 0.13 g PVDF (Sigma-Aldrich, M_w ~250000) (75:15:10 weight ratio) in 2.5 mL NMP (Sigma-Aldrich, anhydrous, 99.5%) using ball milling (PULVERISETTE 7) at 500 rpm for 1 h. Slurry was coated on aluminum foil (15 μm thickness) by doctor blade (250, 265, 280, 300 or 350 μm corresponding to 4.2, 4.5, 4.7, 5, and 5.6 $mg_{KVPFO}\,cm^{-2}$). The film was then dried at 60 °C for 12 h under air. Then, 9.5 mm diameter electrodes were cut out, pressed at 3 tons cm^{-2} (leading to ~36% electrode porosity) and dried again under vacuum at 80 °C for 12 h. At this point, no optimization of the KVPFO electrodes formulation was performed but it will be considered in the future.

Electrochemical experiments

Galvanostatic cycling was conducted using a VMP 3 multichannel system (BioLogic, France) in a 20 °C temperature-controlled room. Two pair cells were assembled for reproducibility while in the results section, data for only one cell is presented for clarity. The electrolyte was 0.8 M KPF_6 (Sigma-Aldrich, ≥99%) EC:DEC (ethylene carbonate, Sigma-Aldrich, ≥99% and diethyl carbonate, Sigma-Aldrich, ≥99%) 1:1 by volume. This electrolyte was selected based on our results of K plating/striping (Figure S1), as discussed in the results section. For half-cells and 3-electrodes cells, i.e., for cells using K metal, a glass fiber membrane (GF/D, from Whatman) was added in contact with the K metal electrode in addition to the two microporous trilayer membranes (PP/PE/PP, from Celgard). The need for a GF/D separator in contact with K metal may be explained by a much better electrolyte wettability of the K surface thanks to the GF/D separator affinity with the K metal compared to a PP/PE/PP separator. This point is further discussed in the result part. In full cells, i.e., without K metal, only the two microporous trilayer membrane (PP/PE/PP, from Celgard) were used. Note that only one PP/PE/PP separator should be necessary but two were used instead as a precaution. For the full-cells assembly, the areal capacities used for both positive and negative electrodes corresponds to the practical capacities obtained experimentally in half-cells, i.e., $Q_{graphite\text{-}practical}$ ~264 mAh g^{-1}, and $Q_{KVPFO\text{-}practical}$ ~82 mAh g^{-1}. Note that in this work, the polarization (ΔV in Figures) was considered as the difference between the average potential in charge (depotassiation) and discharge (potassiation). Thus, in order to assemble reliable K-ion half and full coin-cells (CR2032 316 L were used), different parameters were evaluated as presented in Figure 1.

Before assembling half-cells, the choice of the electrolyte, which is of high importance to control the K plating/stripping performance, was evaluated using K//K symmetric cells.

Then, the optimal electrolyte volume was determined for graphite and KVPFO electrodes in regard to the reversible capacity, coulombic efficiency (CE) and polarization using half-cells. To do so, after and OCV of 1 h, 5 cycles were performed at C/10 between 2–0.01 V and 3.5–5.0 V for graphite (2 $mg_{graphite}\,cm^{-2}$) and KVPFO (5 $mg_{KVPFO}\,cm^{-2}$) electrodes, respectively. The optimal electrolyte volume was then also determined for full KVPFO// graphite cells. To do so, after and OCV of 1 h, 5 cycles were performed at C/10 (vs. KVPFO) between 2–5 V while both negative/positive diameter and capacity ratios of 1.16 (2 $mg_{graphite}\,cm^{-2}$ and 5 $mg_{KVPFO}\,cm^{-2}$) were used.

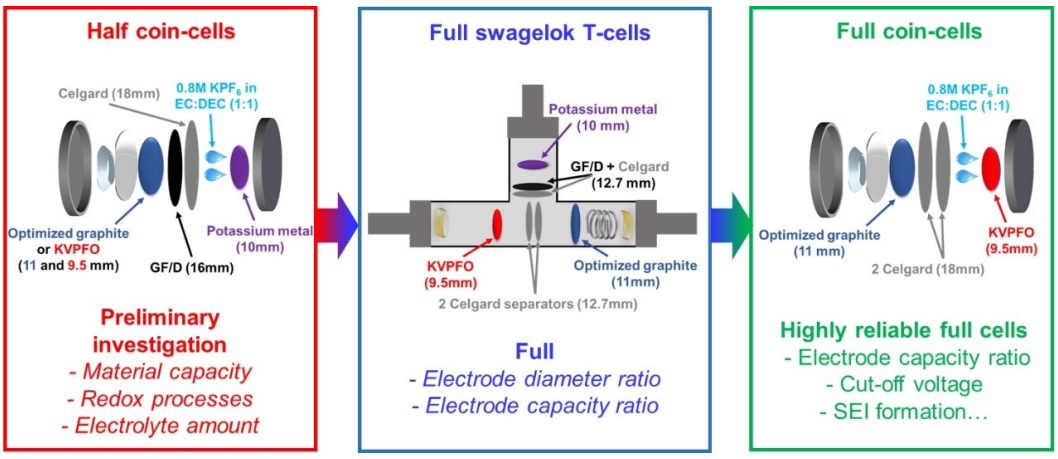

Figure 1. Schematic representation of the approach followed in this work to optimize the assembly of highly reliable K-ion full coin cells.

Second, the optimal graphite/KVPFO diameter ratio (12.7/9.5 and 11/9.5 in mm with 2 $mg_{graphite}\,cm^{-2}$ and 5 $mg_{KVPFO}\,cm^{-2}$ electrodes) was determined in regards to the reversible capacity and CE using 3-electrodes Swagelok T-cells (i.e., full-cells with K metal reference). Note that another 3-electrodes Swagelok cell type was first used in this step, but this cell type was not selected due to some electrolyte reactivity issue (Figure S3), as discussed in the results part. To do so, after an OCV of 1 h, 10 cycles were performed at C/10 (vs. KVPFO) with potential limitations of 3.0–5.0 V, 2–5.0 V and 0.01–2.0 V for E_{KVPFO} (E_{WE}), $E_{KVPFO\text{-}graphite}$ (E_{WE-CE}) and $E_{graphite}$ (E_{CE}), respectively.

Second/third, the optimal graphite/KVPFO capacity ratio (0.98, 1.05, 1.09, 1.16, and 1.30) was determined in regard to the reversible capacity, CE and polarization using both 3-electrodes Swagelok T-cells and full coin-cells. To do so, the loading of the graphite electrode was fixed to 2 $mg_{active\text{-}material}\,cm^{-2}$ while the loading of KVPFO electrode was varied from 4.2 to 5.6 $mg_{active\text{-}material}\,cm^{-2}$ (*i.e.*, 4.2, 4.5, 4.7, 5, and 5.6 corresponding to N/P capacity ratios of 0.98, 1.05, 1.09, 1.16, and 1.30, respectively). For the 3-electrodes Swagelok T-cells, after an OCV of 1 h, 5 cycles were performed at C/10 (vs. KVPFO) with potential limitations of 3.0–5.0 V, 1.2–5.0 V and 0.01–2.5 V for E_{KVPFO} (E_{WE}), $E_{KVPFO\text{-}graphite}$ (E_{WE-CE}) and $E_{graphite}$ (E_{CE}), respectively. For the full coin-cells, after an OCV of 12 h at 40 °C, 50 cycles were performed at C/10 (vs. KVPFO) between 1.2–4.8 V. Note that the reported capacities were calculated based on KVPFO weight. Here, the OCV at 40 °C was found beneficial to the preformation of an SEI, which will the subject of another study. Also, the 1.2–4.8 V voltage windows was selected based on the 3-electrodes results, especially, the 4.8 V upper cut off voltage allows limiting the electrolyte oxidation at high potential.

Finally, full coin-cells with high electrodes loadings (N/P loading ratio of 2/5 and 4/10 $mg_{active\text{-}material}\,cm^{-2}$) were assembled to evaluate the practical energy density for the KVPFO//graphite system. To do so, after an OCV of 12 h at 40 °C, 20 cycles were performed at C/10 (vs. KVPFO) between 2–4.8 V. Importantly, the energy density (in Wh kg_{device}^{-1}) reported in Figure 5 takes into account the mass of both electrodes (including the active materials, carbon additives and binders), the electrolyte and separators.

Results and Discussion

In this study, graphite and KVPFO were selected as active materials for negative and positive electrodes based on their promising electrochemical performance. Indeed, graphite can reversibly intercalate K^+, leading to KC_8, i.e., a theoretical capacity of 279 $mAh\,g^{-1}$.[14] Moreover, some of us recently showed that optimized electrode formulation, i.e., optimized ionic/electronic networks and electrode cohesion/elasticity allows controlling the graphite volume expansion issue, which further increases its interest.[10] Moreover, among the $KVPO_4F_xO_{1-x}$ family, $KVPO_4F_{0.5}O_{0.5}$ (KVPFO) shows the best galvanostatic profile with the lowest polarization, the smoother redox plateaus, the best reversible capacity and CE.[13]

Parameters (separator choice, electrolyte choice and volume) governing half-cells performance

Before assembling full-cells, it is often necessary to first assess active materials performance. To do so, it is important to assemble half-cells with high reproducibility and importantly with negligible impact of the K metal, separator/electrolyte choice/amount. The goal of this part is thus evaluating the parameters governing half-cells performance.

Note first that careful precautions should be taken when preparing K metal electrodes due to its high reactivity even under Ar glovebox atmosphere,[15] so that a specific procedure is proposed in the experimental part. Then, the K metal electrode diameter should always be larger than the working electrode one. Otherwise, using an undersized K metal electrode will limit the delivered capacity and lead to inhomogeneous SEI formation at the working electrode, as previously observed in Li-ion half-cells.[16]

Second, to prevent K dendrites formation, large polarization and low delivered capacity in half-cells, it is mandatory to use a glass fiber separator (noted GF/D or a Solupor membrane;[17] as proposed in the literature) at the K metal electrode side in addition to a Celgard membrane on the working electrode side. This is more likely explained by an electrolyte wettability issue at the K surface induced by the affinity between the separator and K metal. Indeed, Figure S1 shows that graphite// K cells with 2 Celgard membranes delivered only 41 $mAh\,g^{-1}$ during the first discharge at C/20 with a very large polarization of 0.74 mV compared to 269 $mAh\,g^{-1}$ and 0.16 mV when the Celgard at the K metal electrode was replaced by a GF/D separator. The 5th cycle showed an additional polarization increase and thus a capacity decreased with 2 Celgard while nearly no change was observed with the use of a GF/D separator (Figure S1). These results thus highlight the importance of the separator choice when assembling K-ion half-cells.

Third, the electrolyte choice is also of high importance to control the K plating/stripping performance[1] and thus to not alter the delivered capacity, lifetime and power performance of half-cells. In this study, 0.8 M KPF_6 EC:DEC was selected as it showed much lower polarization from low (0.02 $mA\,cm^{-2}$) to moderate (0.8 $mA\,cm^{-2}$) currents among the different electrolytes tested (Figure S2). Overall, as K plating/stripping and thus half-cells performance may vary depending on the selected K metal preparation, separator(s), electrolyte salt(s)/solvent(s) and their purity,[2] it is therefore very important to first determine and select the most suitable combination and not rely only on literature data.

Finally, the electrolyte volume impact on half-cells performance was evaluated (Figure 2) despite that it is usually neglected or not mentioned in the literature. For clarity, Table S1 gather the thickness (μm), porosity (%), diameter (mm) and corresponding porosity volume (μL) for the different components used to assembled K-ion cells in this study, i.e., graphite and KVPFO electrodes, GF/D and Celgard separators as well as the corresponding porosity volume by surface area ($\mu L\,cm^{-2}$). From Table S1, it appears that the electrolyte volume needed in our half-cells to fill

Research Article
doi.org/10.1002/batt.202300061
Chemistry Europe
European Chemical Societies Publishing

both KVPFO or graphite electrode porosity in addition to the separators porosity corresponds to ~17 μL. Electrolyte volume was thus varied from 30 to 100 μL. For KVPFO electrodes, using only 30 μL led to low reversible capacity and no capacity during the 1st and 5th cycles, respectively (Figure 2). Note that the potential jump observed at about 4.5 V is attributed to the redox phenomenon and structural properties of the KVPFO material.[13] Between 50 and 70 μL, similar delivered capacities were observed but using only 50 μL led to much higher polarization, indicating possible ionic limitation even at C/10 cycling rate. Increasing further the electrolyte volume from 70 to 100 μL significantly increased the irreversible capacity associated with the electrolyte oxidation during the 1st cycle between 4 and 4.6 V. This is likely explained by the oxidation of soluble electrolyte degradation species formed at the K metal for which their amount should increase as the electrolyte volume increases. This phenomenon is also supported by the fact that for graphite electrodes, as no oxidation is possible, the same 1st cycle CE was observed as the electrolyte volume was increased. For graphite electrode, increasing the electrolyte volume increased the delivered capacities, especially after 5 cycles due to the large electrolyte consumption to form the SEI. However, no significant change was observed between 70 and 100 μL. To resume, it is thus found that 70 μL is the optimal electrolyte volume for both KVPFO and graphite half-cells with our setup, which is about 4 times higher than the total porosity of the electrodes and separators (~17 μL, Table S1). This result is thus in good agreement with the literature on Li-ion full coin cells assembly that also used an electrolyte volume of about 3.8 times the porosity volume.[18]

Impact of the electrolyte volume on full-cells performance

For full KVPFO//graphite cells, increasing the electrolyte volume from 15 to 50 μL significantly increased the delivered capacity and CE while decreasing the polarization (Figure 2). This indicates a decrease of the ionic limitation due to a better electrode porosity filling by the electrolyte. However, increasing further the electrolyte volume to 70 μL then 100 μL significantly decreased the delivered capacity and CE while increasing the polarization, more likely due to

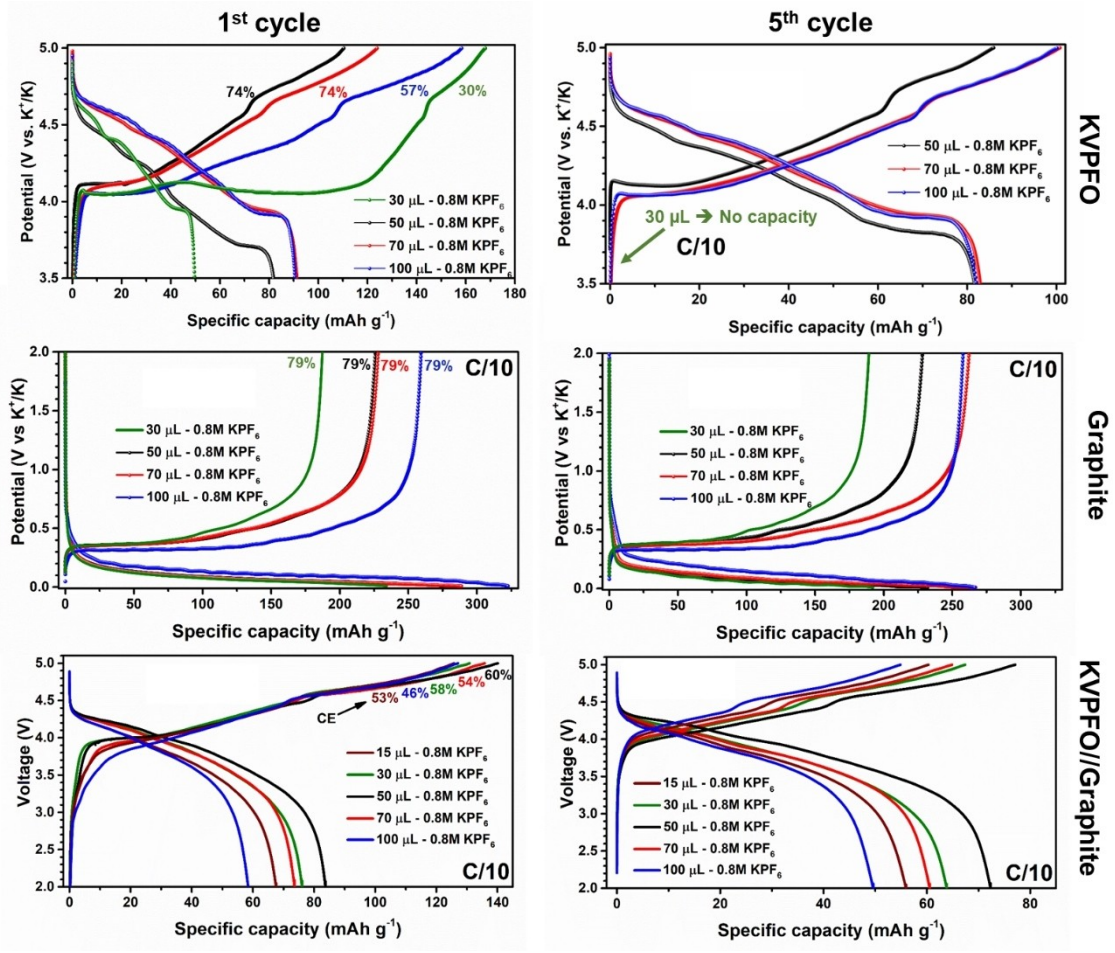

Figure 2. Galvanostatic profiles during the 1st and 5th cycles at C/10 for $KVPO_4F_{0.5}O_{0.5}$//K cells (between 3.5–5 V), graphite//K cells (between 2–0.01 V) and KVPFO//graphite cells (between 2–5 V with both negative/positive diameter and capacity ratios of 1.16) as function of the 0.8 M KPF_6 EC:DEC electrolyte volume as indicated.

Research Article
doi.org/10.1002/batt.202300061
Chemistry Europe
European Chemical Societies Publishing

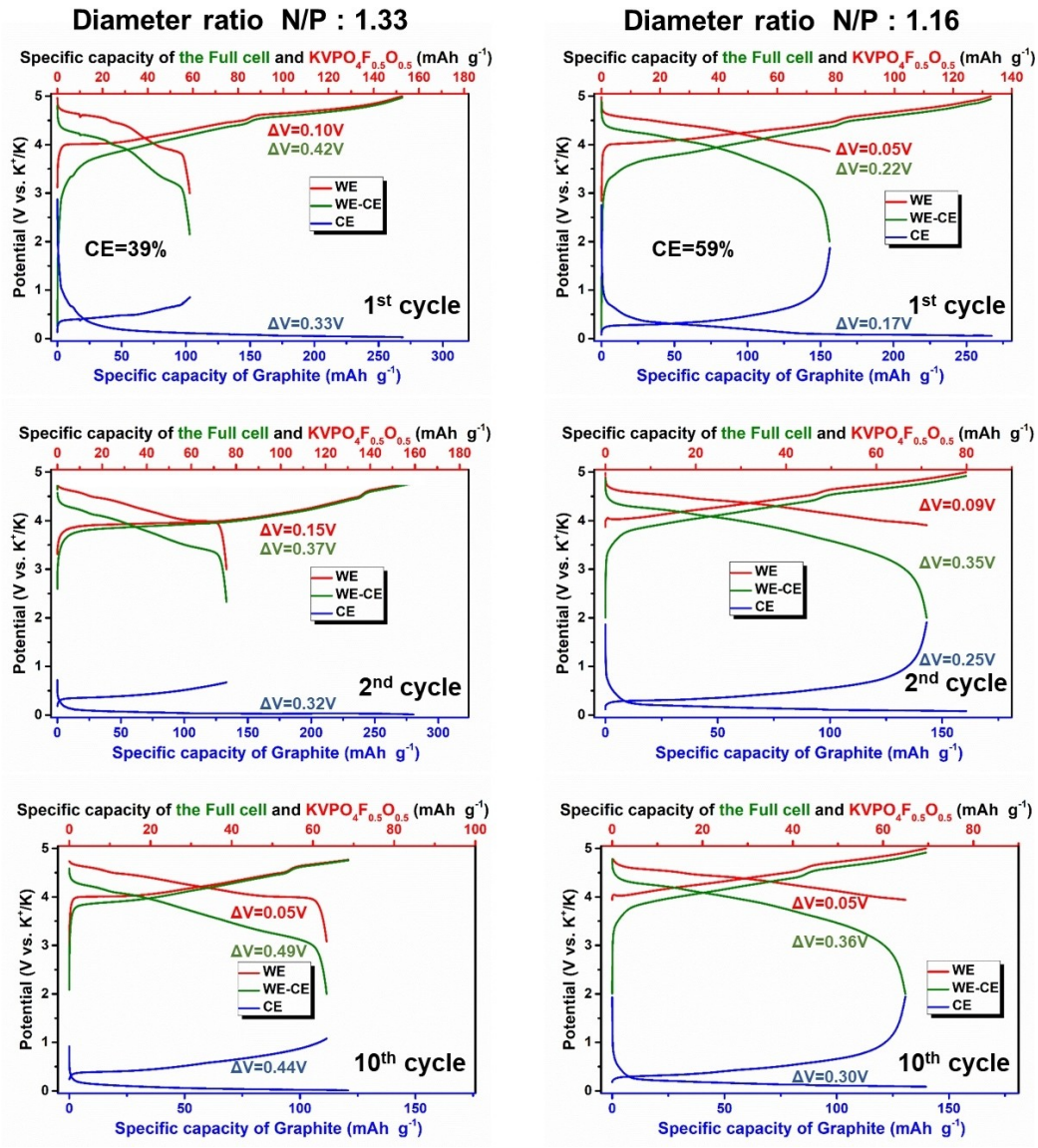

Figure 3. Galvanostatic profiles during the 1st, the 2nd and 10th cycles at C/10 between 3.5–5 V for KVPFO//graphite 3-electrodes T-cells with N/P diameter ratio of 12.7/9.5 = 1.33 and 11/9.5 = 1.16. The graphite/KVPFO capacity ratio was here fixed to 1.16. Note that ΔV corresponds to the polarization, i.e., the difference between the average potentials.

a too high electrolyte degradation and passivation of the electrodes surface by the SEI. To resume, it is thus found that the optimal electrolyte volume for our KVPFO//graphite cells is 50 µL, i.e., about 4 times higher than the total porosity of the electrodes and separators (Table S1), similarly to what was found previously for our half-cells. Note that for the 3-electrodes T-cell study presented after, 100 µL of electrolyte was also used which correspond to ~4 times the total porosity of the electrodes and separators (Table S1). Overall, these results highlight that an optimal electrolyte volume should be determined to maximize the delivered capacity, polarization, CE and capacity retention while keeping in mind that excess of electrolyte should be limited in regard to commercial cells.

Impact of the negative/positive diameter on full-cells performance

In this part, 3-electrodes cells were used to evaluate the impact of the negative/positive (N/P) diameter and capacity ratios on the delivered capacity and CE. Note that the optimization of both N/P ratios could have been done using only 2-electrode cells but the interest of 3-electrodes cells is to gain insight on the limiting electrode and the associated phenomenon. To do so, large Swagelok cells were first used but unfortunately it led to high electrolyte degradation with coloration of the K metal reference electrode with such cell design (Figure S3). In addition, a yellow color was observed on the separator in contact with the K metal, indicating a possible contamination of the reference electrode (not showed). As an alternative, smaller

Research Article
doi.org/10.1002/batt.202300061
Chemistry Europe
European Chemical Societies Publishing

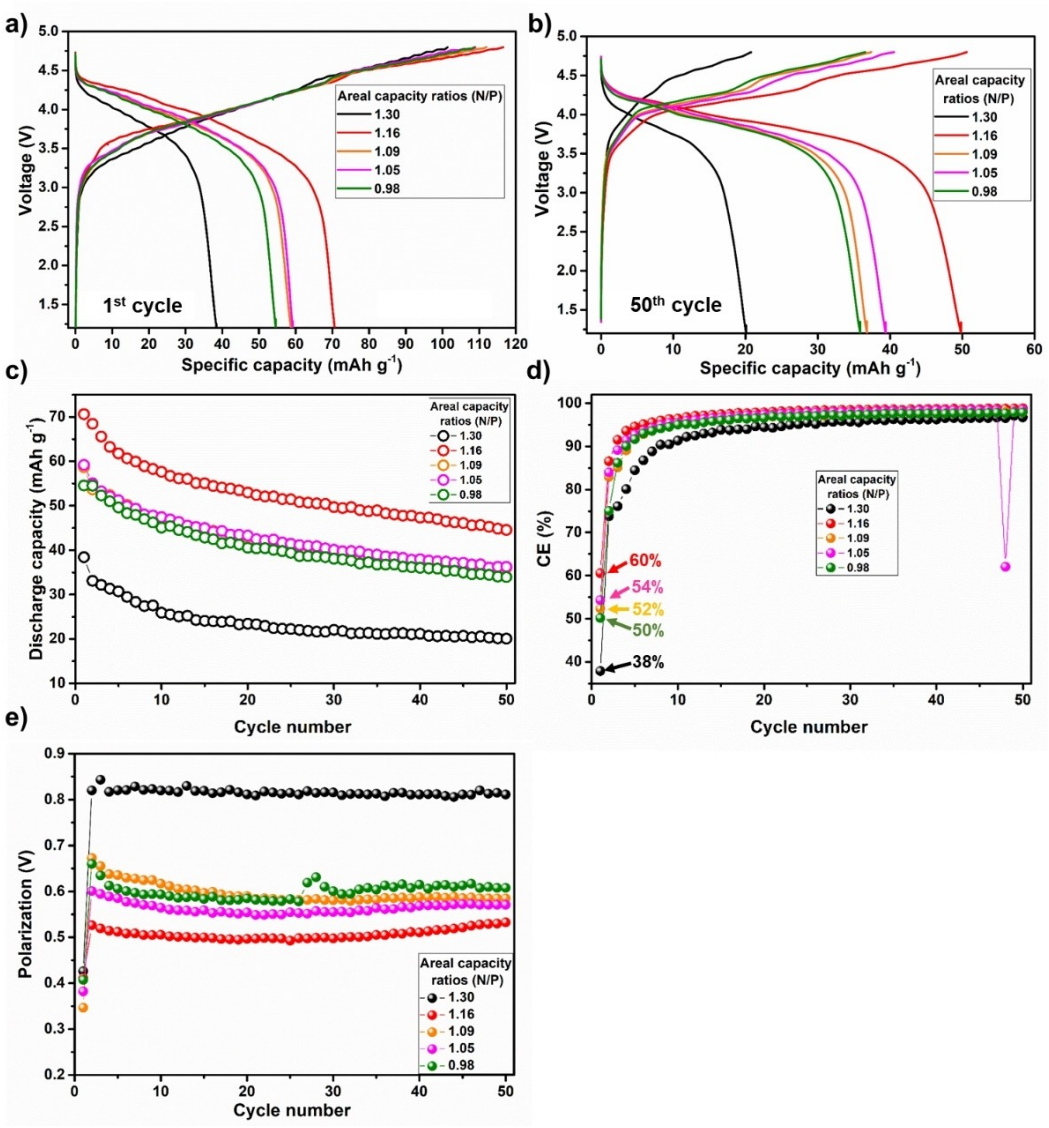

Figure 4. a) 1st and b) 50th galvanostatic cycles profiles between 1.2–4.8 V at C/10 for KVPFO//graphite full coin-cells as function of the capacity ratio. c) Capacity retention, d) coulombic efficiency and e) polarization for the same cells over 50 cycles. The graphite/KVPFO diameter ratio was here fixed to 1.16. Note that the reported capacities were calculated based on KVPFO weight.

Swagelok cells with a T-configuration (K metal placed perpendicularly to the other electrodes) was used with the previously optimized electrolyte volume (100 μL, Table S1). This highlights the importance of the 3-electrodes cell design for KIBs.

The impact of the graphite/KVPFO diameter ratio was then evaluated with the Swagelok T-cells (Figure 3). While using a large diameter ratio of 1.33 (12.7 mm /9.5 mm) may help for the electrode alignment during cell assembly, it also significantly increased the irreversible capacity (61%) associated with the electrolyte degradation as well as the electrodes/cell polarizations. Indeed, from cycles 2 to 10, the KVPFO electrode could not reach its 5 V cut-off voltage due to a much higher electrolyte degradation between 3.9 and 4.5 V. This is more likely explained by the excess of graphite that needs to passivate and thus produces excess of soluble electrolyte degradation species that migrate to the KVPFO electrode where they are oxidized. Indeed, for N/P = 1.16, this phenomenon is almost supressed. After 10 cycles, the KVPFO and graphite electrodes delivered only 62 and 115 mAh g^{-1}, respectively. When the graphite electrode diameter was decreased to 11 mm, corresponding to a N/P diameter ratio of 1.16, the 5 V cut-off voltage of KVPFO was always reached so that both KVPFO and graphite electrodes delivered higher capacity of 66 and 131 mAh g^{-1} after 10 cycles, corresponding to a full-cell capacity of 66 mAh g^{-1} with an average potential of 3.8 V. Overall, while it might be possible to optimize further (i.e., to decrease further) the N/P diameter ratio, a value of 1.16 ± 0.2 is here found satisfying.

Research Article
doi.org/10.1002/batt.202300061
Chemistry Europe
European Chemical Societies Publishing

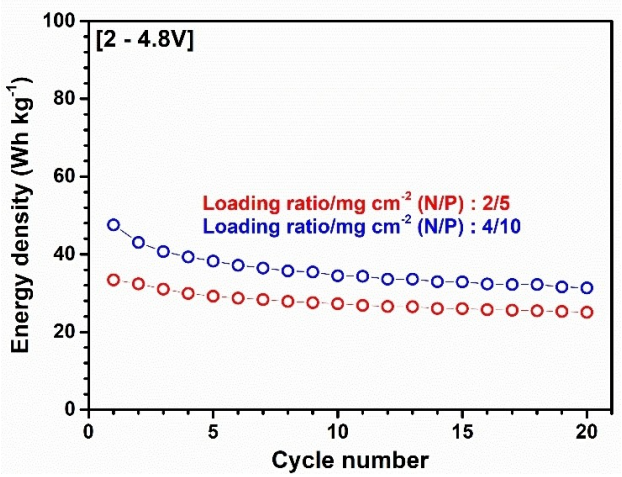

Figure 5. Energy density as function of the cycle number for KVPFO// graphite full coin-cells with N/P loading ratio of 2/5 and 4/10 (in $mg_{active\text{-}material}\,cm^{-2}$) as obtained during cycling between 2–4.8 V at C/10. The diameter and capacity ratios were here both fixed to 1.16. Note that the energy density in $Wh\,kg_{device}^{-1}$ takes into account the mass of both electrodes (including the active materials, carbon additives and binders), the electrolyte and separators.

Impact of the negative/positive diameter on full-cells performance and capacity ratios in full-cells

The impact of the graphite/KVPFO capacity ratio was then evaluated in full coin-cells (Figure 4) and supported by Swagelok T-cells results (Figure S4). Note that here, full coin-cells cycling was performed at C/10 between 1.2–4.8 V after optimization of the voltage limits. The corresponding results will, however, be published in an upcoming study together with SEI analysis. Overall, the N/P capacity ratio of 1.16 led to the highest 1st cycle capacity (71 $mAh\,g^{-1}$) and CE (60%), the best capacity retention over 50 cycles (70% with 50 $mAh\,g^{-1}$) with the lowest polarization (0.53 V after 50 cycles, Figure 4). Indeed, for a lower N/P capacity ratio of 1.06, the 3-electrodes cell analysis showed that the cells are limited by the excess of KVPFO so that the voltage limit of 5 V couldn't be reached during few cycles while the graphite was fully utilized (Figure S4a). At the opposite, using a higher N/P capacity ratio of 1.3 led to a full utilization of the KVPFO electrode (Figure S4b). However, a very large irreversible capacity was observed (Figure S4b) due to the excess of graphite that need to be passivated by the electrolyte degradation/SEI formation (similarly to the use of a large N/P diameter ratio previously, Figure 3). Also, it leads to high oxidation between 4 and 4.5 V due to the oxidation of excess of soluble electrolyte degradation species formed at the graphite electrode (Figure S4b). Thus, using low and high N/P capacity ratio leads to cells limited by the KVPFO and graphite electrodes, respectively.

Optimized KVPFO//graphite full cells with high loading

In this part, the optimized N/P diameter and capacity ratios were used to assembled KVPFO//graphite coin-cells with high energy, i.e., with high electrodes loadings. Overall, Figure 5 shows that increasing the N/P loading ratio from 2/5 to 4/10 (in $mg_{active\text{-}material}\,cm^{-2}$) allowed reaching an energy density of about 47 $Wh\,kg^{-1}$ with a retention of 68% after 20 cycles. To our knowledge, this result is probably the highest reported so far in the K-ion full-cells literature especially considering the high electrodes loading used. Finally, if pouch cells can be constructed with a N/P loading of 4/10 (in $mg\,cm^{-2}$), an optimized KVPFO electrodes formulation (i.e., at least with 90/5/5 wt.% of KVPFO/carbon/PVDF) and a practical electrolyte volume (1.2 times the total porosity instead of 4 times in coin cells), the energy density could reach about 80 $Wh\,kg^{-1}$. This will of course need to be confirmed in the future.

Conclusion

This work demonstrates approaches to assemble reliable K-ion half- and full-cells. Using graphite and $KVPO_4F_{0.5}O_{0.5}$ based electrodes, it is first illustrated that the separators choice/number and electrolyte choice/volume are key parameters governing half-cells performance. For instance, a glass fiber membrane (GF/D, from Whatman) needs to be added in contact with K metal to optimize the delivered capacity and limit the polarization. Importantly, for both half- and full-cells the electrolyte volume should be fixed to about 4 times the porosity volume of both binder and electrode also to optimize the delivered capacity, CE and polarization. Based on these results and using 3-electrodes cells, the optimal negative/positive (N/P) diameter ratio then the optimal N/P capacity ratio are determined to be 1.16 ± 0.2. Note that the design of the 3-electrodes cells is also important. Finally, following these approaches, KVPFO// graphite coin-cells with a high N/P loading ratio of 4/10 (in $mg_{active\text{-}material}\,cm^{-2}$) were assembled, leading to cells with an energy density of about 47 $Wh\,kg_{device}^{-1}$. Note that if further improvement can be obtained, such as the KVPFO electrode optimization and the use of pouch cells with lower electrolyte volume, the energy density of KVPFO//graphite cells could reach about 80 $Wh\,kg^{-1}$, making K-ion cells promising in the future if sufficient lifetime is obtained. Overall, the approaches followed in this work can be used as a guide to assemble any KIBs full-cell system with high reproducibility and reliability, which is more representative of the practical performance than half-cells. This work should thus help determining the best negative/positive materials combination to accelerate the development of high energy and high power KIBs.

Acknowledgements

This work was part of the TROPIC project supported by Agence Nationale de la Recherche (ANR) under the grant ANR-19-CE05-0026. Authors thank Laure Monconduit and Lorenzo Stievano for the fruitful discussions. Lénaïc Madec would also like to thank Patrick Soudan for the 3-electrodes Swagelok cells and discussion about cells setup.

Conflict of Interest

The authors declare no conflict of interest.

Data Availability Statement

The data that support the findings of this study are available from the corresponding author upon reasonable request.

Keywords: full cells · graphite · half-cells · $KVPO_4F_{0.5}O_{0.5}$ · parameters optimization

[1] N. Xiao, W. D. McCulloch, Y. Wu, *J. Am. Chem. Soc.* **2017**, *139*, 9475–9478.
[2] K. Kubota, M. Dahbi, T. Hosaka, S. Kumakura, S. Komaba, *Chem. Rec.* **2018**, *18*, 1–22.
[3] J. Touja, V. Gabaudan, F. Farina, S. Cavaliere, L. Caracciolo, L. Madec, H. Martinez, A. Boulaoued, J. Wallenstein, P. Johansson, L. Stievano, L. Monconduit, *Electrochim. Acta* **2020**, *362*, 137125.
[4] L. Caracciolo, L. Madec, G. Gachot, H. Martinez, *ACS Appl. Mater. Interfaces* **2021**, *13*, 57505–57513.
[5] J. Zhang, Z. Cao, L. Zhou, G. T. Park, L. Cavallo, L. Wang, H. N. Alshareef, Y. K. Sun, J. Ming, *ACS Energy Lett.* **2020**, *5*, 3124–3131.
[6] Q. Li, Z. Cao, W. Wahyudi, G. Liu, G. T. Park, L. Cavallo, T. D. Anthopoulos, L. Wang, Y. K. Sun, H. N. Alshareef, J. Ming, *ACS Energy Lett.* **2021**, *6*, 69–78.
[7] T. Hosaka, K. Kubota, H. Kojima, S. Komaba, *Chem. Commun.* **2018**, *54*, 8387–8390.
[8] J. Touja, P. N. Le Pham, N. Louvain, L. Monconduit, L. Stievano, *Chem. Commun.* **2020**, *56*, 14673–14676.
[9] J. Xie, J. Li, W. Zhuo, W. Mai, *Mater. Today* **2020**, *6*, 100035.
[10] B. Larhrib, L. Madec, L. Monconduit, H. Martinez, *Electrochim. Acta* **2022**, *425*, 140747.
[11] L. Madec, V. Gabaudan, G. Gachot, L. Stievano, L. Monconduit, H. Martinez, *ACS Appl. Mater. Interfaces* **2018**, *10*, 34116–34122.
[12] F. Allgayer, J. Maibach, F. Jeschull, *ACS Appl. Energ. Mater.* **2022**, *5*, 1136–1148.
[13] R. Wernert, L. H. B. Nguyen, E. Petit, P. S. Camacho, A. Iadecola, A. Longo, F. Fauth, L. Stievano, L. Monconduit, D. Carlier, L. Croguennec, *Chem. Mater.* **2022**, *34*, 4523.
[14] S. Komaba, T. Hasegawa, M. Dahbi, K. Kubota, *Electrochem. Commun.* **2015**, *60*, 172–175.
[15] T. Hosaka, S. Muratsubaki, K. Kubota, H. Onuma, S. Komaba, *J. Phys. Chem. Lett.* **2019**, *10*, 3296–3300.
[16] L. Madec, H. Martinez, *Electrochem. Commun.* **2018**, *90*, 61–64.
[17] A. J. Naylor, M. Carboni, M. Valvo, R. Younesi, *ACS Appl. Mater. Interfaces* **2019**, *11*, 45636–45645.
[18] V. Murray, D. S. Hall, J. R. Dahn, *J. Electrochem. Soc.* **2019**, *166*, A329–A333.

Manuscript received: February 21, 2023
Revised manuscript received: March 13, 2023
Accepted manuscript online: March 15, 2023
Version of record online: April 12, 2023